GEOPHYSICS, VOL. 51, NO. 4 (APRIL 1986); P. 972-983, 13 FIGS.

Analysis of multiple-source bipole-quadripole resistivity surveys using the apparent resistivity tensor

H. M. Bibby*

ABSTRACT

Measurements of apparent resistivity made using the bipole-dipole method depend upon the location and orientation of the current source relative to the body under study. Although it has been recognized that this dependence on orientation can be partially overcome by use of two current bipoles with different orientations, no agreement on the method of analysis of multiple source surveys has been reached. The most general form of presentation of such results is an apparent resistivity tensor. Various rotation invariants derived from the apparent resistivity tensor can be regarded as mean values of apparent resistivity, independent of the direction of the electric field, thus greatly reducing the "false anomalies" typical of single-source bipole-dipole survey results. Two of the tensor invariants obey the principle of reciprocity: if the roles of the current and potential electrodes are interchanged, the invariants are unchanged.

The properties of the apparent resistivity tensor are demonstrated for selected simple models. For a horizontally layered medium, when the receiver array is far from the current source, the tensor is symmetric and has invariants which depend only on the distance from the current source. The extreme values of apparent resistivity occur when the electric field vector is tangential and radial relative to the current source. These extreme values correspond to the Schlumberger apparent resistivity and the "polar" dipole apparent resistivity, respectively.

Lateral discontinuities in resistivity are modeled with both a single vertical discontinuity and a hemispherical model. The source-dependent variations in the apparent resistivity derived from a single-current bipole are greatly reduced in plots of the tensor invariants. For a vertical discontinuity, the tensor trace (the sum of the diagonal elements) is close to the resistivity underlying the receiver site, whereas for a hemisphere, the square root of the tensor determinant gives the best representation. Near lateral discontinuities in resistivity, the apparent resistivity tensor indicates strong dependence of apparent resistivity on the direction of the measured electric field. This apparent anisotropy can be used as an indicator of such discontinuities, yielding both position and orientation of the discontinuity.

INTRODUCTION

Although the technique of measuring apparent resistivity using more than one bipole current source has been used for many years (e.g., Risk et al., 1970), the debate continues on how to combine results from distinct current sources in a unique manner to give the most diagnostic representation of results. The most general form of presenting such results is in use of an apparent resistivity tensor (Bibby, 1977). Since it was first suggested, considerable work has been done in New Zealand using this method to analyze multiple-current source bipole survey results in geothermal regions (Bibby et al., 1984, Risk et al., 1984), and a number of the early surveys made in the Central Volcanic Region of New Zealand have been reanalyzed. To aid the understanding of the tensor representation and to show its advantages, several simple models of resistivity distribution are examined here. The tensor representation of multiple-current source surveys greatly reduces the problems of the dependence of apparent resistivity on the orientation of the current bipoles. Furthermore, particular rotational invariants of the tensor can be used to highlight particular features, such as the position and orientation of a resistivity discontinuity.

BACKGROUND

One of the earliest descriptions of noncollinear dipole-dipole arrays was given in Al'pin (1950). The system described consisted of a single, short current dipole as source, with the potential field monitored by a pair of potential electrodes at a remote location aligned at some known orientation relative to the current dipole. Choices of arrays were named for their particular orientation, such as polar, equatorial, radial, azimuthal, parallel, and perpendicular. In actual field use, how-

Manuscript received by the Editor April 17, 1985; revised manuscript received September 11, 1985.
*Geophysics Division, D.S.I.R., P.O. Box 1320, Wellington, New Zealand.

ever, it is seldom possible to make the current dipole short enough for it to be considered a close approximation to an idealized dipole source, for which the current electrode separation must be small compared with the distance between the source and receiver. This limitation was recognized by Zohdy (Zohdy and Jackson, 1969; Zohdy, 1970) who introduced the more generalized form in which the current was assumed to be finite (i.e., a bipole). Zohdy termed this array the "bipole-dipole array."

Both of these single-receiver systems have severe limitations. Small inhomogeneities in resistivity can produce a rotation of the electric field from that over a horizontally layered medium. Consequently, the apparent resistivity calculated for a single component of the electric field can be misleading (Frohlich, 1968). The next major refinement to the technique was introduced by Risk et al. (1970) who measured two perpendicular components of the electric field, from which both the magnitude and the direction of the electric field (i.e., the electric field vector) can be derived. The "total-field" apparent resistivity was defined using the magnitude of the measured electric field alone. All the resistivities corresponding to the multitude of special four-electrode arrays (differing only by the orientation of the potential array) can be derived from this total-field measurement. While the original use of the simple dipole array was in resistivity depth soundings (e.g., Anderson and Keller, 1966), the bipole-quadripole array has been used principally for detection of lateral resistivity variations and in this capacity the technique has been applied to geothermal exploration (Risk et al., 1970; Bibby and Risk, 1973; Keller et al., 1975; Stanley et al., 1976).

Even when the total field is measured, the bipole-quadripole technique is not free from the influence of the orientation of the current source with respect to inhomogeneities. Work with model calculations of apparent resistivity has shown that complex patterns of apparent resistivity can occur even over simple structures. Furthermore, false anomalies apparently unrelated to the causative structure can occur in regions where the model resistivity is constant. Simple models studied have included vertical contacts and dikes (Keller et al., 1975), horizontal layering (Zohdy, 1978), hemispheroidal sinks (Bibby and Risk, 1973), and a buried conducting sphere (Singh and Espindola, 1976). Numerical solutions for more complex models were given in Beyer (1977), Dey and Morrison (1977), and Hohmann and Jiracek (1979). The pattern of apparent resistivity and the position of false anomalies for all simple structures depend upon the orientation of the current bipole with respect to the structure being investigated. As with the problem of the dependence of the apparent resistivity on the orientation of a single-receiver dipole, the dependence of apparent resistivity on the current source orientation can be dealt with by using a pair of near-orthogonal current sources. This type of surveying is termed "multiple-source bipole-quadripole" surveying to distinguish it from single-source surveying. The term covers both use of four-current electrodes, forming a pair of mutually perpendicular current sources, and the triad of current electrodes introduced in Risk et al. (1970) which are used a pair at a time to form three current sources.

Although use of multiple-current sources is now common practice, considerable variation is still seen in the presentation of the results of such surveys. Doicin (1976) investigated use of quadripole current sources, and advocated using a single mean value of apparent resistivity based on the vector cross product of the electric fields. An alternate approach, used by Keller and Furgerson (1977), was described as the "rotating dipole method" in which the components of the measured electric fields from each bipole source are added vectorially and the resultant vector is rotated by using appropriate current strengths to derive a mean value of the apparent resistivity.

A more general method of analyzing multiple-source bipole-quadripole surveys is presented here using a tensor representation of apparent resistivity (Bibby, 1977). Rotational invariants of the tensor are related to the parameters advocated in Doicin (1976) and to those derived from the rotating dipole method. The properties of the tensor can be diagrammed in several ways, and presented so as to emphasize some particular characteristic of the body under study.

NOTATION AND DEFINITIONS

Definitions of apparent resistivity involving bipole-dipole arrays are simply expressed in terms of two vector fields: the measured electric field vector **E**, and the (theoretical) current density vector **J** which would be generated by the same current source in a half-space of uniform electrical resistivity.

In a bipole-dipole survey, although the current bipole length may not be small compared with the distance from the current bipole to the measurement point, the lengths of the measuring dipoles are much smaller than either. Thus, the measured potential differences between each pair of nearly perpendicular dipoles enables the electric field vector **E** to be determined (see, for example, Bibby and Risk, 1973; Zohdy, 1978). The current density **J**, on the other hand, is a theoretical quantity and depends only on the geometry and the current in the source bipole. For a current bipole AB (Figure 1) with current I, the current density at a point P can be expressed as

$$\mathbf{J}_{AB} = (\mathbf{r}_a/r_a^3 - \mathbf{r}_b/r_b^3)I/2\pi, \tag{1}$$

where $\mathbf{r}_a$ and $\mathbf{r}_b$ are the position vectors of P relative to current electrodes A and B, respectively. From equation (1) the magnitude of $\mathbf{J}_{AB}$ is

$$|\mathbf{J}_{AB}| = (r_a^{-4} + r_b^{-4} - 2r_a^{-2}r_b^{-2}\cos\alpha)^{1/2}I/2\pi, \tag{2}$$

where α is the angle between lines AP and BP (Figure 1).

A number of definitions of apparent resistivity exist for the bipole-dipole array, but they can all be written as the ratio of

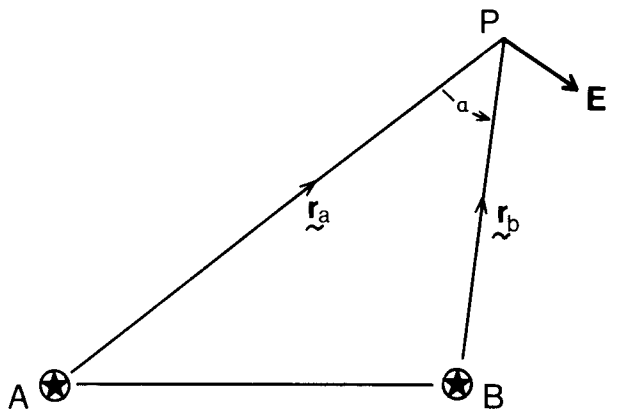

FIG. 1. For current bipole AB, the position of field station P is defined by the vectors $\mathbf{r}_a$ or $\mathbf{r}_b$. The electric field **E** is measured at P.

the magnitude of the electric field vector (or a selected component) to the magnitude of the current density (or some component). The multiplicity of definitions arises because in general **E** and **J** are not parallel, nor is there any reason to expect them to be parallel in a nonhomogeneous earth. Zohdy (1978), for example, gave three possible definitions which can be expressed as

$$\rho_a = |\mathbf{E}_{AB}|/|\mathbf{J}_{AB}|, \tag{3a}$$

$$\bar{\rho}_E = |\mathbf{E}_{AB}|^2/\mathbf{E}_{AB}\cdot\mathbf{J}_{AB}, \tag{3b}$$

and

$$\bar{\rho}_{E_0} = \mathbf{E}_{AB}\cdot\mathbf{J}_{AB}/|\mathbf{J}_{AB}|^2, \tag{3c}$$

which differ according to whether magnitudes only are compared [equation (3a)], the component of the current density in the direction of the electric field is used [equation (3b)], or the component of the electric field in the direction of the current density is used [equation (3c)]. The total-field apparent resistivity given by equation (3a) is most commonly used.

The apparent resistivity tensor

The complete relationship between two vector fields can be expressed in terms of a tensor quantity. Thus, the most general relationship between the nonparallel electric and current density vectors in the horizontal plane is in the form of an apparent resistivity tensor $\underset{\sim}{\rho}$ given by

$$\mathbf{E} = \underset{\sim}{\rho}\mathbf{J}. \tag{4a}$$

$\underset{\sim}{\rho}$ consists of four independent elements which are generally all nonzero, i.e.,

$$\underset{\sim}{\rho} = \begin{bmatrix} \rho_{11} & \rho_{12} \\ \rho_{21} & \rho_{22} \end{bmatrix}. \tag{4b}$$

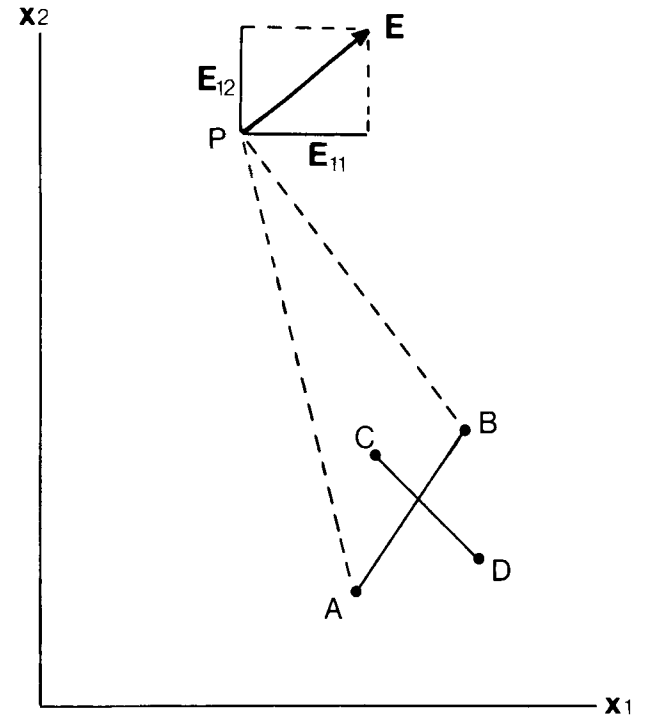

FIG. 2. The components of the electric field vector $\mathbf{E}_{AB}$ for current source AB are taken as E_{11} and E_{12} as shown. Components E_{21} and E_{22} are defined similarly for source CD.

Equation (4a) has a similar form to Ohm's law for an anisotropic material, although the apparent resistivity tensor generally is not symmetric. The analogy with Ohm's law when **E** and **J** are nonparallel suggests that the apparent resistivity can be regarded as anisotropic at each site.

For just a single current bipole, not enough information is available to determine all four tensor components. However, when multiple current sources are used, and a measure of **E** is made for each source, the apparent resistivity tensor can be determined.

The concept of an apparent resistivity tensor approach to bipole-quadripole resistivity measurements was introduced in Bibby (1977). The components of the apparent resistivity tensor can be readily expressed in terms of the components of **E** and **J** for each of the current bipoles. Consider arbitrarily oriented Cartesian coordinates (x_1, x_2), and for the bipole source AB (Figure 2) let the components of the measured electric field $\mathbf{E}_{AB}$ be (E_{11}, E_{12}). The corresponding components of the current density derived from equation (2) are taken as (J_{11}, J_{12}). Similarly, for the source CD the components of the electric field $\mathbf{E}_{CD}$ and current density $\mathbf{J}_{CD}$ are taken as (E_{21}, E_{22}) and (J_{21}, J_{22}), respectively. Substituting each pair in equation (4) and solving for $\underset{\sim}{\rho}$ gives

$$\underset{\sim}{\rho} = \begin{pmatrix} E_{11}J_{22} - E_{21}J_{12} & E_{21}J_{11} - E_{11}J_{21} \\ E_{12}J_{22} - E_{22}J_{12} & E_{22}J_{11} - E_{12}J_{21} \end{pmatrix} \Big/ |\mathbf{J}_{AB}\times\mathbf{J}_{CD}|, \tag{5}$$

where the magnitude of the vector cross-product is

$$|\mathbf{J}_{AB}\times\mathbf{J}_{CD}| = J_{11}J_{22} - J_{21}J_{12}.$$

Because the derivation of the four components of $\underset{\sim}{\rho}$ uses all the information available from the two measurements of the electric field, it is possible to derive from $\underset{\sim}{\rho}$ the value of the apparent resistivity for any single-component system (arrays such as the parallel, perpendicular etc.), as well as the total-field apparent resistivity for each source independently. The generalized form can thus be used to derive the apparent resistivity for any specialized (and necessarily less general) definition.

PROPERTIES OF THE APPARENT RESISTIVITY TENSOR

The values of the components of $\underset{\sim}{\rho}$ given by equation (5) are dependent upon the orientation of the coordinate axes chosen for the computation and hence are not necessarily the most convenient representation. For a nonsymmetric second-rank tensor there are three independent combinations of the components which are not dependent upon the coordinate axes (the rotational invariants). In addition, any combination of these invariants is also an invariant (although not an independent one). The three invariants can be chosen as

$$P_1 = \tfrac{1}{2}(\rho_{11} + \rho_{22}) = \tfrac{1}{2}\,\text{trace}\,(\underset{\sim}{\rho}), \tag{6}$$

$$P_2 = (\rho_{11}\rho_{22} - \rho_{12}\rho_{21})^{1/2} = [\text{determinant}\,(\underset{\sim}{\rho})]^{1/2}, \tag{7}$$

and

$$P_3 = \tfrac{1}{2}(\rho_{12} - \rho_{21}). \tag{8}$$

Each of these invariants has the dimension of resistivity, although their ratios (nondimensional) are also invariant and can be used as alternative means of presentation.

The invariants can be written in terms of the original components of **E** and **J** using equation (5). For example,

$$P_2 = |\mathbf{E}_{AB} \times \mathbf{E}_{CD}|/|\mathbf{J}_{AB} \times \mathbf{J}_{CD}|. \quad (9)$$

This is the definition of apparent resistivity suggested in Doicin (1976).

An alternative form of the apparent resistivity tensor, useful in pictorially representing the tensor, is obtained by splitting the tensor into symmetric and asymmetric parts (Bibby, 1977)

$$\underset{\sim}{\rho} = \Pi_1 \begin{pmatrix} \cos 2\alpha & \sin 2\alpha \\ \sin 2\alpha & -\cos 2\alpha \end{pmatrix} + \Pi_2 \begin{pmatrix} \cos 2\beta & \sin 2\beta \\ -\sin 2\beta & \cos 2\beta \end{pmatrix}, \quad (10)$$

where

$$\Pi_1 = \tfrac{1}{2}[(\rho_{11} - \rho_{22})^2 + (\rho_{12} + \rho_{21})^2]^{1/2} = [P_1^2 + P_3^2 - P_2^2]^{1/2}, \quad (11)$$

$$\Pi_2 = \tfrac{1}{2}[(\rho_{11} + \rho_{22})^2 + (\rho_{12} - \rho_{21})^2]^{1/2} = [P_1^2 + P_3^2]^{1/2}, \quad (12)$$

$$\tan 2\alpha = (\rho_{12} + \rho_{21})/(\rho_{11} - \rho_{22}), \quad (13)$$

and

$$\tan 2\beta = (\rho_{12} - \rho_{21})/(\rho_{11} + \rho_{22}) = P_3/P_1. \quad (14)$$

Because Π_1, Π_2, and β can be expressed in terms of rotational invariants, they are invariants and will not be changed by a change in coordinate axes.

The angle α is the azimuth of the principal axis of the symmetric tensor relative to the coordinate axes and is not a rotational invariant because any change of axes will produce a corresponding change in α. The asymmetric portion of the tensor represents a rotation, characterized by the angle 2β. In terms of the current density and electric field vector, 2β is the overall rotation of the measured electric field $\mathbf{E}$ relative to the theoretical current density $\mathbf{J}$.

Reciprocity

For any four-electrode configuration used for measuring electrical resistivity, the principle of reciprocity states that no change will occur in the measured voltage if the roles of the current and potential electrodes are interchanged, and equal current is applied (Wenner, 1912; Keller and Frischknecht, 1966). When applied to resistivity prospecting (e.g., Habberjam, 1967) this means the apparent resistivity measured with two pairs of electrodes is independent of which pair is used as the current source. This principle can be extended readily to a multiple-source bipole-quadripole configuration where, if the roles of the current and potential quadripoles are interchanged, the invariants P_1 and P_2 remain unchanged and the principle of reciprocity is upheld. The third invariant, P_3, which represents the rotation of the current density field relative to the electric field, depends upon the dimensions and orientations of each array and does not exhibit reciprocity. Proof of this extended principle follows from the four-electrode reciprocity principle and definitions given in equations (5) to (8).

Graphical representation

The apparent resistivity tensor is derived from two measurements of the electric field $\mathbf{E}_{AB}$ and $\mathbf{E}_{CD}$ corresponding to each of two current sources. However, any linear combination of the current sources, say $p\mathbf{J}_{AB} + q\mathbf{J}_{CD}$, where p, q are arbitrary scalars, could also be used to define an apparent resistivity appropriate to some other direction of the current density vector. The corresponding electric field would be the same linear combination of the electric fields, i.e.,

$$p\mathbf{E}_{AB} + q\mathbf{E}_{CD}.$$

Because for each source the electric field and current density are related by $\underset{\sim}{\rho}$, any linear combination will also satisfy the same equation, so that

$$p\mathbf{E}_{AB} + q\mathbf{E}_{CD} = \underset{\sim}{\rho}(p\mathbf{J}_{AB} + q\mathbf{J}_{CD}). \quad (15)$$

For each linear combination, a total-field apparent resistivity can be defined in the form of equation (3a)

$$\rho_a = |p\mathbf{E}_{AB} + q\mathbf{E}_{CD}|/|p\mathbf{J}_{AB} + q\mathbf{J}_{CD}|. \quad (16)$$

By varying p and q, an apparent resistivity can be defined corresponding to any direction of $\mathbf{E}$ or $\mathbf{J}$. Such an approach can be made directly by using the apparent resistivity tensor.

Taking the current density vector to be of magnitude J in direction θ, relative to the given coordinates, i.e.,

$$\mathbf{J}_\theta = \begin{bmatrix} J\cos\theta \\ J\sin\theta \end{bmatrix},$$

along with equation (4) and $\underset{\sim}{\rho}$ given in equation (10), the corresponding electric field vector is

$$\mathbf{E}_\theta = \begin{bmatrix} \Pi_1 \cos(2\alpha - \theta) + \Pi_2 \cos(2\beta - \theta) \\ \Pi_1 \sin(2\alpha - \theta) - \Pi_2 \sin(2\beta - \theta) \end{bmatrix}. \quad (17)$$

Similarly, if the electric field is given by

$$\mathbf{E}_\phi = \begin{bmatrix} E\cos\phi \\ E\sin\phi \end{bmatrix}$$

the corresponding current density is

$$\mathbf{J}_\phi = E/(\Pi_2^2 - \Pi_1^2) \begin{bmatrix} \Pi_2 \cos(2\beta + \phi) - \Pi_1 \cos(2\alpha - \phi) \\ \Pi_2 \sin(2\beta + \phi) - \Pi_1 \sin(2\alpha - \phi) \end{bmatrix}. \quad (18)$$

Substituting into equation (3a) gives the total-field apparent resistivity ρ_ϕ corresponding to the electric field vector in direction ϕ:

$$\rho_\phi = |\mathbf{E}_\phi|/|\mathbf{J}_\phi| = (\Pi_2^2 - \Pi_1^2)[\Pi_1^2 + \Pi_2^2 - 2\Pi_1\Pi_2 \cos(2\beta + 2\phi - 2\alpha)]^{-1/2}. \quad (19)$$

Equation (19) can be written in a more convenient form by putting

$$\Pi_1 + \Pi_2 = a,$$

and

$$\Pi_2 - \Pi_1 = b.$$

Rearranging terms, ρ_ϕ satisfies the relationship

$$\rho_\phi^2 \cos^2(\phi + \beta - \alpha)/a^2 + \rho_\phi^2 \sin^2(\phi + \beta - \alpha)/b^2 = 1 \quad (20)$$

which is the equation for an ellipse in polar coordinates (ρ_ϕ, ϕ), semimajor axis a, semiminor axis b, with the major axis lying along the line

$$\phi = \alpha - \beta. \quad (21)$$

That is, plotting the value of the total-field apparent resistivity

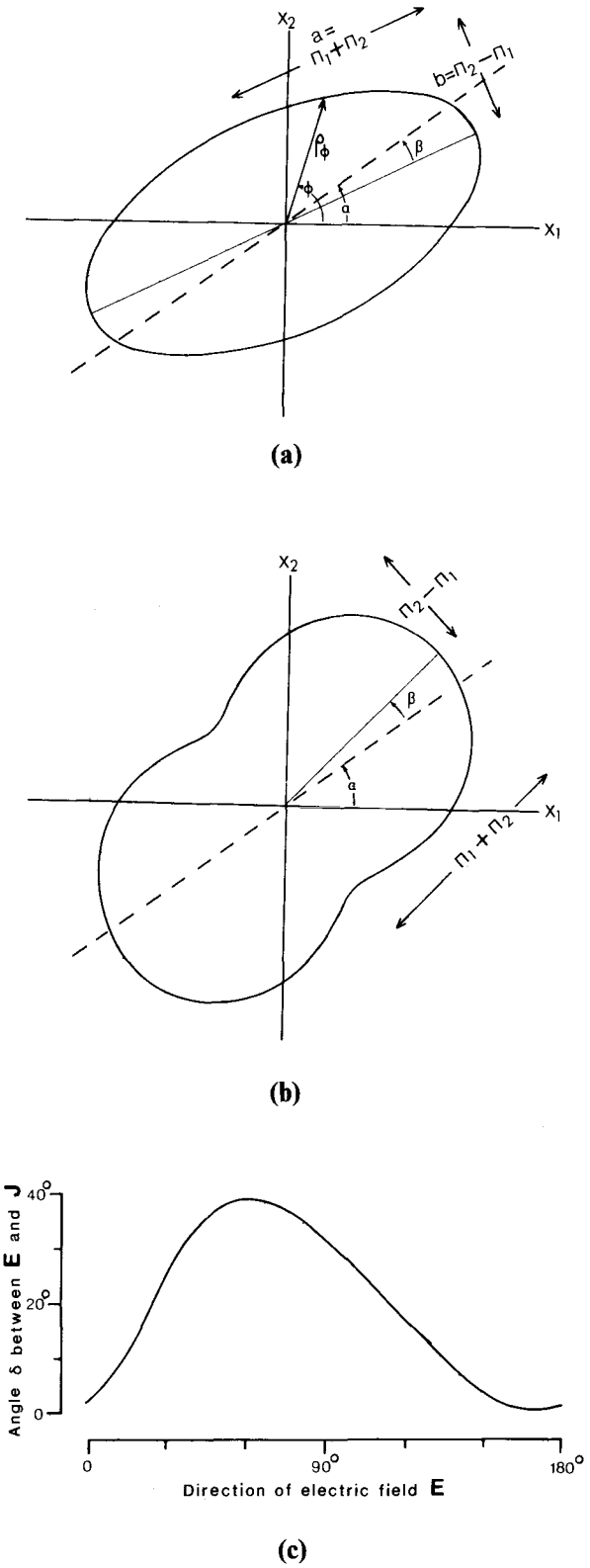

FIG. 3. The total-field apparent resistivity plotted in the direction of (a) the electric field vector and (b) the current density vector. The parameters used in this example are $\alpha = 35$ degrees, $\beta = 10$ degrees, and $\Pi_2/\Pi_1 = 3$. For (a) the figure is an ellipse, major axis in the direction $(\alpha - \beta)$ with the ratio of semimajor to semiminor axes 2 : 1. For (b) the maximum resistivity occurs when **J** is in direction $(\alpha + \beta)$. (c) The deviation δ of the direction of the electric field vector from that in a uniform half-space, for the example above. The mean value of the deviation is 2β (20 degrees).

in the direction of the electric field traces out an ellipse. This elliptical representation of the apparent resistivity was used in Morris (1978). An example of one such ellipse is given in Figure 3a.

The ellipse can be used to visualize some of the invariants of the apparent resistivity tensor. The area of the ellipse is

$$\pi ab = \pi(\Pi_2^2 - \Pi_1^2) \tag{22}$$

$$= \pi P_2^2. \tag{23}$$

Thus P_2 is the radius of the circle that has an area equal to that of the ellipse, and it can be regarded as one measure of an average apparent resistivity.

Because the apparent resistivity varies with direction, a coefficient of apparent anisotropy can be defined by

$$\lambda_a = (a/b)^{1/2} \tag{24}$$

$$= (\Pi_2 + \Pi_1)/P_2. \tag{25}$$

The values and orientation of the maximum and minimum apparent resistivities, a and b, are a useful diagnostic tool in the interpretation of survey results and are used in this paper to represent the ellipse.

The relationships given can be used to relate the rotating dipole method of presenting multiple-source survey results (Tasci, 1975; Keller and Furgerson, 1977; Morris, 1978) to the tensor parameters. Harthill (1978) and Morris (1978) both used an average apparent resistivity $\bar{\rho}$ defined by the arithmetic mean of the extreme values of the total-field apparent resistivity, i.e.,

$$\bar{\rho} = (a + b)/2$$

$$= \Pi_2.$$

This parameter is also an invariant of the apparent resistivity tensor. A method of calculating the extremes from the field data was given in Morris (1978), although earlier authors (e.g., Tasci, 1975) computed ρ_ϕ for a selection of values of ϕ and chose the extremes by inspection.

The total-field apparent resistivity ρ_θ can also be derived in terms of θ, the direction of the current density vector. From equation (17),

$$\rho_\theta = [\Pi_1^2 + \Pi_2^2 + 2\Pi_1\Pi_2 \cos(2\theta - 2\alpha - 2\beta)]^{1/2}. \tag{26}$$

The resulting hyperellipse, plotted in Figure 3b, has the same extreme values as the ellipse of Figure 3a. The maximum value occurs when the current density lies in the azimuth $\theta_m = \alpha + \beta$, while the corresponding electric field lies at azimuth $\alpha - \beta$. Thus at the extreme values of total-field apparent resistivity, the angle between the current density for a uniform half-space and the measured electric field vector **E** is 2β, with the direction of the principal axis bisecting them. The angle β is thus a measure of the mean rotation of the measured electric field relative to the current density for a uniform half-space. Generally, the angle δ between **E** and **J** is given by

$$\tan\delta = |\mathbf{E} \times \mathbf{J}|/\mathbf{E} \cdot \mathbf{J} \tag{27}$$

$$= \frac{\Pi_2 \sin 2\beta - \Pi_1 \sin(2\alpha - 2\phi)}{\Pi_2 \cos 2\beta - \Pi_1 \cos(2\alpha - 2\phi)}, \tag{28}$$

where the electric field is in the direction ϕ. This is dependent upon ϕ for all but the special case when $\Pi_1 = 0$. Figure 3c shows an example of the variation of the deviation δ with the direction of the electric field.

HORIZONTALLY LAYERED MEDIUM

When dealing with a horizontally layered medium, it is useful to represent the medium not by the resistivities of the medium, but by the corresponding apparent resistivity of the Schlumberger sounding curve. Zohdy (1978), in his comprehensive discussion of the bipole-quadripole method applied to horizontally layered media, pointed out that the electric field resulting from a single current source can be written in terms of the Schlumberger apparent resistivity $\rho_s(r)$ at spacing r. Thus the electric field at a distance r from a current source of strength I is

$$\mathbf{E}(r) = I\rho_s(r)\mathbf{r}/2\pi r^3. \tag{29}$$

Hence, for a current bipole AB, the electric field is

$$\mathbf{E}_{AB} = I[\rho_s(r_a)\mathbf{r}_a/r_a^3 - \rho_s(r_b)\mathbf{r}_b/r_b^3]/2\pi. \tag{30}$$

Equation (30) can be separated to give the Schlumberger apparent resistivities for each separate current source. Taking the vector cross-product with $\mathbf{r}_a$ gives

$$|\mathbf{E}_{AB} \times \mathbf{r}_a| = I\rho_s(r_a)|\mathbf{r}_a \times \mathbf{r}_b|/2\pi r_b^3 \tag{31}$$

or

$$\rho_s(r_a) = 2\pi r_b^3|\mathbf{E}_{AB} \times \mathbf{r}_a|/|\mathbf{r}_a \times \mathbf{r}_b|I. \tag{32}$$

Similarly, taking the vector cross-product with $\mathbf{r}_b$ gives

$$\rho_s(r_b) = 2\pi r_a^3|\mathbf{E}_{AB} \times \mathbf{r}_b|/|\mathbf{r}_a \times \mathbf{r}_b|I. \tag{33}$$

Writing the vector cross-products in terms of their components in the appropriate system, these reduce to the form given in Zohdy (1978) [his equations (38) and (39)].

Using Zohdy's method, it is possible to derive the Schlumberger resistivity for spacings equivalent to each of the separations r_a and r_b from any measurement of the electric field using a bipole source. However, as the spacing increases, the vectors $\mathbf{r}_a$ and $\mathbf{r}_b$ tend to become parallel and nearly equal in magnitude, and the separation of $\mathbf{E}_{AB}$ into the parts produced by each electrode [equations (32) and (33)] becomes highly sensitive to any small variations caused by local resistivity variations. In practice this method becomes unstable at large distances.

For close spacings, multiple-source bipole-quadripole survey results can be treated by considering each source independently to give equivalent Schlumberger apparent resistivities (Zohdy's method). At large distances, however, when this method becomes unstable, the tensor apparent resistivity takes a particularly convenient form.

In the limiting case when r_a and r_b become large, each current source can be approximated by a dipole of finite moment. Choosing polar coordinates centered on the current dipole (Figure 4), the components of the electric field (E_r, E_θ) can be derived from equation (31) in the limit as r_a and r_b become large (see also Al'pin, 1950)

$$E_r = 2b\cos\theta[\rho_s(r) - \tfrac{1}{2}r\partial\rho_s(r)/\partial r]/r^3$$

and (34)

$$E_\theta = b\sin\theta\rho_s(r)/r^3,$$

where b is the dipole moment (AB I) and θ is the orientation relative to the current dipole. The current density of a uniform half-space in these coordinates has components

$$J_r = 2b\cos\theta/r^3$$

and (35)

$$J_\theta = b\sin\theta/r^3.$$

For a pair of current sources with the same center the apparent resistivity tensor in these polar coordinates is simply

$$\underset{\sim}{\rho} = \begin{bmatrix} \rho_s(r) - \tfrac{1}{2}r\partial\rho_s(r)/\partial r & 0 \\ 0 & \rho_s(r) \end{bmatrix}. \tag{36}$$

Because the tensor is symmetric, β is zero. The maximum and minimum values of apparent resistivity always occur when the electric field is aligned along the radial and tangential axes where the values are $\rho_s(r) - \frac{1}{2}r(\partial\rho_s/\partial r)$ and $\rho_s(r)$, respectively. These values were derived in Al'pin (1950) for the "polar" and "equatorial" dipole arrays, respectively. Which of the radial or tangential directions has the greatest apparent resistivity depends upon the slope of the sounding curve; when the Schlumberger apparent resistivity is increasing, the maximum is along the radial line, and when the curve is descending, the maximum occurs in the tangential direction. From the extremes, both the Schlumberger resistivity and the gradient of the sounding curve can be derived directly.

For a horizontally layered medium, contour maps of apparent resistivity derived for a single bipole source take a characteristic peanut shape (Zohdy, 1978). Outside the immediate vicinity of the electrodes, however, the tensor invariants depend only upon the distance from the source, and not upon the orientation, and thus they will produce circular contours.

A horizontally layered structure will be characterized (outside the immediate vicinity of the current source) by an apparent resistivity tensor which (1) is symmetric (i.e., $\beta = 0$), (2) has its maximum and minimum values corresponding to the electric field perpendicular and parallel to the line from the source to the receiver, (3) has invariants which depend only on the distance from the source and when mapped will contour as circles, and (4) from which the Schlumberger sounding curve and its gradient can be derived.

VERTICAL RESISTIVITY DISCONTINUITY

It is possible to consider the changes that occur in the apparent resistivity tensor in the immediate vicinity of a vertical resistivity discontinuity without considering a specific detailed model. To satisfy the boundary conditions on the electric field as a vertical discontinuity between regions of resistivity ρ_1 and

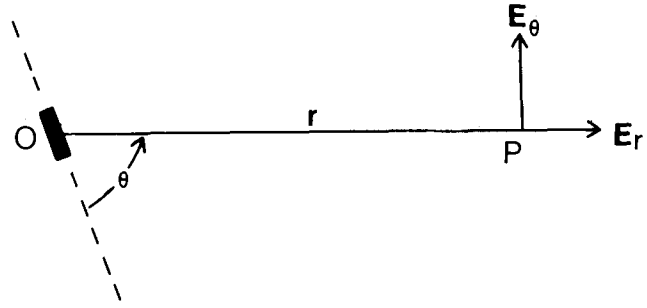

FIG. 4. The radial (E_r) and tangential (E_θ) components of the electric field vector for an idealized bipole at O. The field position is given in radial coordinates (r, θ).

ρ_2 is crossed, the component of the electric field perpendicular to the boundary is discontinuous by a factor equal to the resistivity contrast ρ_2/ρ_1, while the component of the electric field parallel to the boundary is continuous. Taking coordinate axes perpendicular and parallel to the discontinuity in resistivity, let $\underset{\sim}{\rho}$ be the apparent resistivity tensor an infinitesimal distance from the discontinuity in the region of resistivity ρ_1. To satisfy the boundary conditions, a point at a very small distance on the other side of the boundary must have an apparent resistivity tensor

$$\underset{\sim}{\rho}' = \begin{bmatrix} (\rho_2/\rho_1)\rho_{11} & (\rho_2/\rho_1)\rho_{12} \\ \rho_{21} & \rho_{22} \end{bmatrix}. \tag{37}$$

The change in the P_2 invariant across the boundary follows directly from equation (7):

$$P'_2 = (\rho_2/\rho_1)^{1/2} P_2.$$

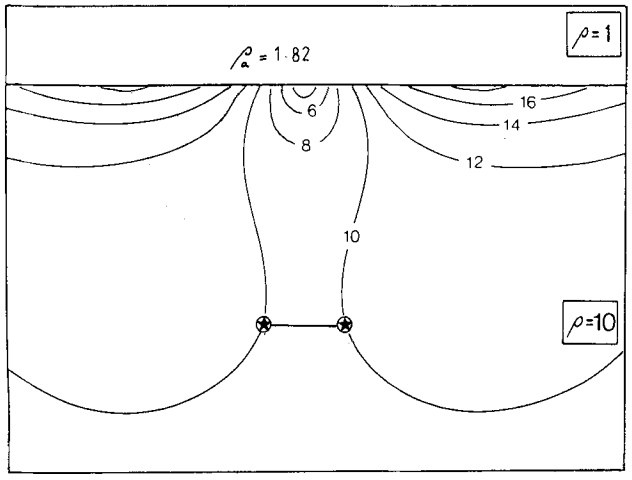

(a)

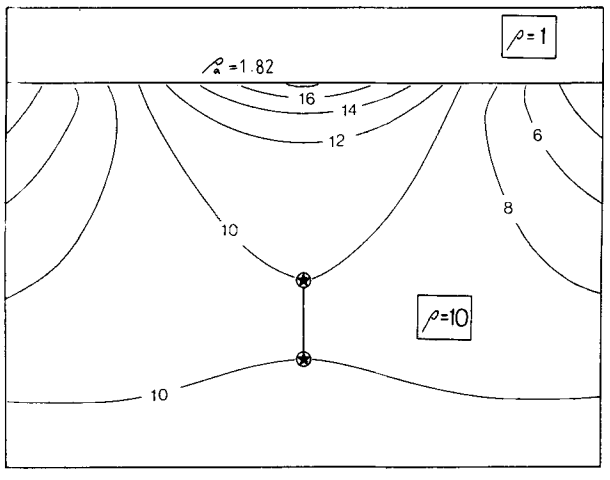

(b)

FIG. 5. Contours of the total-field apparent resistivity for a current bipole parallel (a) and perpendicular (b) to a vertical discontinuity of resistivity, with resistivity contrast 10 : 1. Current electrodes (situated in the high-resistivity zone) are shown by stars.

For a large resistivity contrast, the contrast in two components of the tensor tends to produce large changes in the apparent anisotropy near such a discontinuity; large apparent anisotropy is characteristic of the resistivity tensor near a vertical resistivity discontinuity. The difference in the apparent resistivity tensors across a vertical discontinuity $\Delta\underset{\sim}{\rho} = \underset{\sim}{\rho} - \underset{\sim}{\rho}'$ also has a characteristic form, with a maximum value perpendicular to the discontinuity and a zero minimum value.

As an example of a vertical discontinuity, consider the model of a half-space separating two regions of contrasting resistivity. Aspects of multiple source-bipole surveying for this model were discussed in Doicin (1976) and Keller and Furgerson (1977). Figure 5 shows contour maps of apparent resistivity for a bipole current source parallel (Figure 5a) and perpendicular (Figure 5b) to a discontinuity of resistivity with a contrast of 10 : 1 across the discontinuity. The effect of orientation of a single-bipole source on the resulting pattern of total field apparent resistivity is clearly brought out by this model. Within the region which contains the current sources, large variations of apparent resistivity occur, with values ranging from one-fifth to nearly twice the actual resistivity in the vicinity of the measuring site. Such variations occur for any source orientation, although the location of the false anomalies varies with the orientation of the current source relative to the discontinuity.

For a plane discontinuity, the electric field vector in the region not containing the current electrodes (resistivity ρ_2) is simply $2\rho_2/(\rho_1 + \rho_2)$ times the electric field in a uniform half-space of resistivity ρ_1 (the resistivity at the current electrodes) (for example, Van Nostrand and Cook, 1966). Thus, in this region the total-field bipole-quadripole apparent resistivity is constant with a value

$$\rho_a = 2\rho_1\rho_2/(\rho_1 + \rho_2), \tag{38}$$

independent of the orientation of the current source. Because the electric field is a constant multiple of the current density vector for a uniform half-space in this region, the apparent resistivity tensor $\underset{\sim}{\rho}'$ is also constant throughout this region, viz.,

$$\underset{\sim}{\rho}' = 2\rho_1\rho_2/(\rho_1 + \rho_2)\begin{bmatrix} 1 & 0 \\ 0 & 1 \end{bmatrix}. \tag{39}$$

From equation (37), the apparent resistivity tensor an infinitesimal distance from the boundary on the current electrode side is

$$\underset{\sim}{\rho} = 2\rho_1\rho_2/(\rho_1 + \rho_2)\begin{bmatrix} (\rho_1/\rho_2) & 0 \\ 0 & 1 \end{bmatrix}, \tag{40}$$

where coordinates are chosen perpendicular and parallel to the discontinuity. This applies at all points along the boundary and is independent of the orientation of either current bipole and independent of the distance of the current sources from the boundary.

The invariants and other properties can be deduced from equation (40). Near the boundary the maximum value occurs when the electric field is either parallel ($\rho_1 < \rho_2$) or perpendicular ($\rho_1 > \rho_2$) to the discontinuity as the boundary is crossed. Furthermore, the ratio of maximum to minimum is equal to the resistivity contrast.

Thus the extreme values can indicate the discontinuity, giving both the resistivity contrast and the orientation of the boundary. Figure 6 shows a plot of the maximum and mini-

mum values of the resistivity tensor (i.e., the major and minor axes of the elliptical representation of the tensor) derived from the two bipole sources of Figures 5a and 5b. The magnitudes of the extremes are indicated by the length of the bar drawn in the direction of the corresponding electric field.

As the boundary is approached, the apparent anisotropy increases, reaching its maximum at the discontinuity. At the same time the orientation of the major axis of the apparent resistivity ellipse systematically changes as the boundary is approached so that the major axis becomes perpendicular to the boundary. This characteristic of the axes of the ellipse can be used to identify resistivity discontinuities.

If the resistivity increases across the discontinuity, the maximum value of apparent resistivity occurs when the electric field is parallel to the boundary. The greatest contrast in apparent resistivity across the boundary still occurs when the electric field is perpendicular to the boundary. That is, the discontinuity occurs in the minimum apparent resistivity, while the maximum apparent resistivity varies smoothly.

Various forms of the invariants for the multiple source configuration (derived from the sources of Figures 5a and 5b) can be used to give "averaged" apparent resistivity at each site, or to emphasize particular features, for example, the apparent anisotropy. In particular, Figure 7a shows the invariant P_2. At the boundary P_2 can be derived from equation (40)

$$P_2 = 2\rho_1(\rho_1\rho_2)^{1/2}/(\rho_1 + \rho_2).$$

The contrast across the discontinuity is $(\rho_1/\rho_2)^{1/2}$ ($10^{1/2}$ for the case shown). The false anomalies which occurred in the apparent resistivity derived from each current bipole independently (Figure 5) were eliminated, and away from the boundary zone P_2 more realistically reflects the resistivity beneath the site.

The other estimates of average apparent resistivity are P_1 and Π_2, which are identical when $\beta = 0$. P_1 is contoured in Figure 7b. From equation (40), as the boundary is approached, the value of P_1 becomes

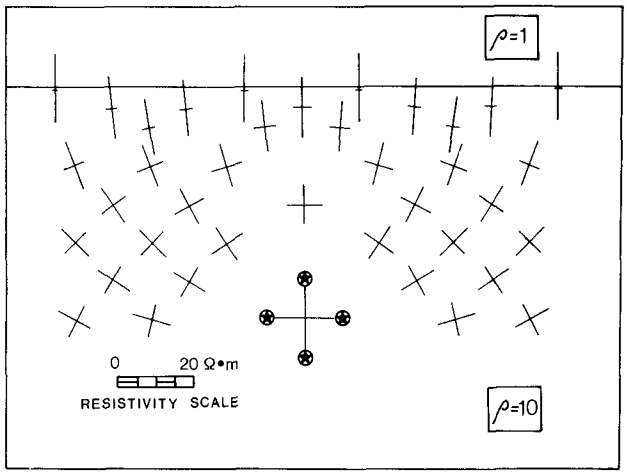

FIG. 6. Extrema of the apparent resistivity tensor for the multiple-bipole source shown in the presence of a vertical discontinuity in apparent resistivity. The maximum and minimum resistivities are plotted in the direction of the corresponding electric field vector, with the magnitude of the apparent resistivity given by the length of the bar.

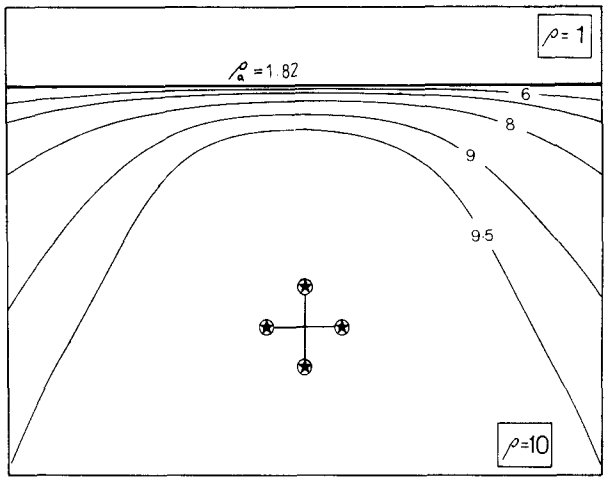

(a)

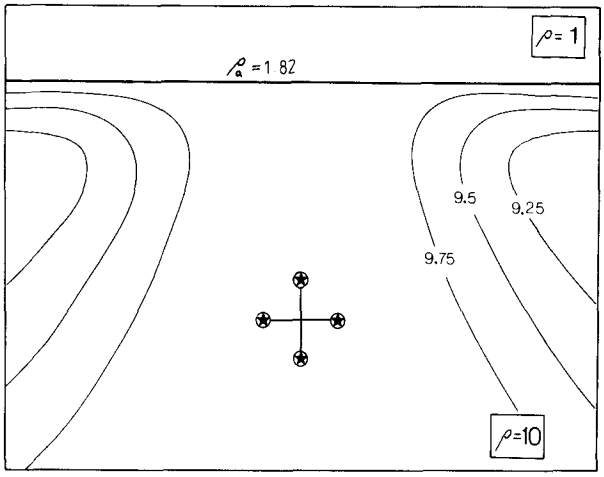

(b)

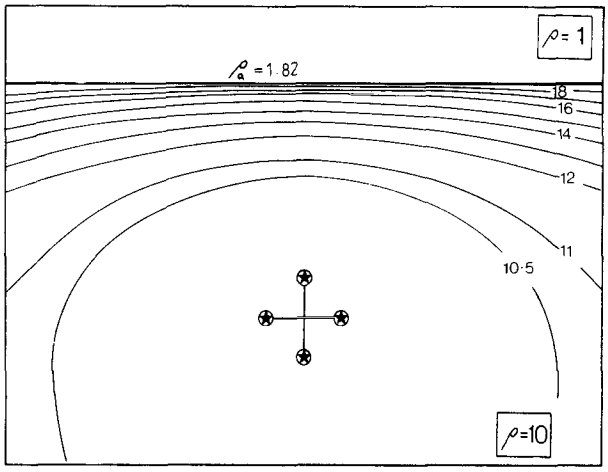

(c)

FIG. 7. Tensor invariants for a multiple-current bipole source in the presence of a single vertical resistivity discontinuity. (a) P_2 invariant (in $\Omega \cdot m$). (b) P_1 invariant (in $\Omega \cdot m$). (c) Maximum value of total-field apparent resistivity derived from the apparent resistivity tensor. Note that the greatest values occur at the discontinuity.

$$P_1 = \Pi_2 = (\rho_1/\rho_2 + 1)\rho_1\rho_2/(\rho_1 + \rho_2)$$
$$= \rho_1.$$

Thus, on the current electrode side of the discontinuity, as the boundary is approached, P_1 takes a value equal to the resistivity of that region. Throughout this region the invariant P_2 is within 10 percent of ρ_1.

Choosing an appropriate tensor invariant emphasizes a particular feature of any study. For example, in this case the boundary is characterized by high apparent anisotropy in its vicinity. The greatest contrast across the boundary occurs in the maximum apparent resistivity (see Figure 7c), although in emphasizing the resistivity contrast, the maximum apparent resistivities do not reflect the resistivity below the measurement site.

HEMISPHERICAL SINK

As an example of a slightly more complex resistivity distribution, consider the apparent resistivity measured with a multiple-source bipole-quadripole survey in the presence of a hemisphere of contrasting resistivity. The apparent resistivities for this model were computed by G. F. Risk (pers. comm.) from an explicit solution for the potential given in Van Nostrand and Cook (1966). The particular model chosen is a hemisphere of resistivity 1 $\Omega \cdot$ m embedded in a half-space of resistivity 10 $\Omega \cdot$ m with individual current source bipoles lying outside the hemisphere, along polar and equatorial axes relative to the hemisphere. Contour maps of the total-field apparent resistivity for each source bipole are shown in Figures 8 and 9. Within the hemisphere the total-field apparent resistivity is almost constant and shows little variation in magnitude as the orientation of the source bipole varies. However, outside the hemisphere large variations can occur. For both current bipoles the contrast in apparent resistivity across the boundary ranges from unity up to the actual resistivity contrast (10 times), depending upon the direction of the electric field relative to the discontinuity. From either survey it would be difficult to distinguish the real resistivity variations from the complex pattern of false anomalies, with apparent resistivities in some locations being more than three times the resistivity beneath the potential electrodes. Note, however, that within the hemisphere the apparent resistivity is almost independent of the source bipole orientation suggesting only slight apparent anisotropy.

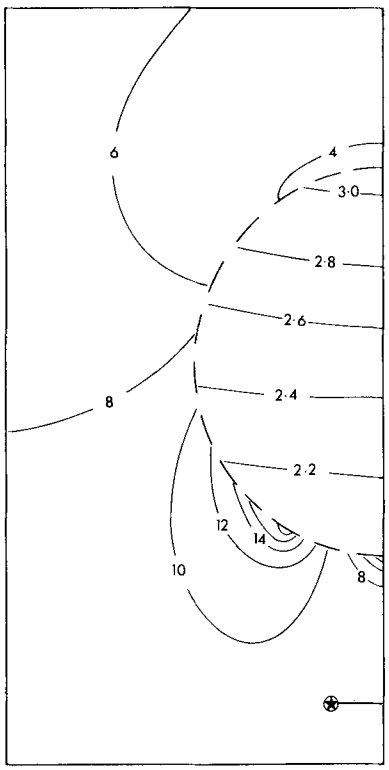

FIG. 8. Contours of the total-field bipole-dipole apparent resistivity ($\Omega \cdot$ m) near a hemispherical sink for the bipole source placed equatorially with respect to the hemisphere. The model shown is for a hemisphere of resistivity of 1 $\Omega \cdot$ m embedded in a uniform resistivity of 10 $\Omega \cdot$ m. The pattern is symmetrical about the diameter through the center of the current bipole, and so only one half is shown. The boundary of the hemisphere is shown by the dashed curves, and the positions of the current electrodes are shown by the stars joined by solid lines.

Combining the data from each of these source bipoles, the apparent resistivity tensor at each point was computed, and the invariants were derived. The invariants P_1 and P_2 which both represent mean values of the tensor, are shown in Figures 10 and 11. In the case of a vertical discontinuity, the invariant P_1 gave the best representation of actual resistivity in the region containing the current electrodes. For the hemisphere, however, although P_1 (Figure 10) gives a good estimate of the resistivity on the near side of the hemisphere, on the far side the apparent resistivity reaches values of 17 $\Omega \cdot$ m in the shadow zone behind the hemisphere. Despite these high values, the invariant is a better representation than either of the individual bipole contour maps.

The tensor invariant P_2 shown in Figure 11 is a much better representation of the resistivity beneath the potential electrodes than in the case of a vertical discontinuity. The greatest variation occurs on the line of symmetry along which the edge of the hemisphere behaves in a similar way to a plane vertical contact. A comparison of Figure 11 with Figures 8 and 9 shows how use of the tensor invariants obtained from multiple-source data has almost eliminated the false anomalies that occurred for the single-bipole results.

The invariant Π_2, also used as a mean value of apparent resistivity, is related to P_1 by

$$P_1 = \Pi_2 \cos 2\beta.$$

For the hemisphere the rotational invariant β, shown in Figure 12, has values of less than 6 degrees, making contours of P_1 and Π_2 almost indistinguishable and either form could have been used. The pattern of variation of β is not diagnostic, and although discontinuities occur at the boundary, they are small. For the example shown, symmetry requires that β is zero along the central axis, and that on opposite sides of this axis, β will be of equal magnitude, but opposite sign. The greatest values occur toward the rear of the hemisphere, where the presence of the hemisphere will produce large deviations of the electric field from the direction in a uniform medium.

Within the low-resistivity hemisphere, the apparent resistivities measured with each current bipole are nearly equal; consequently, the apparent resistivity tensor shows little apparent anisotropy in this region. In practice, when there is only small apparent anisotropy, small irregularities in resistivi-

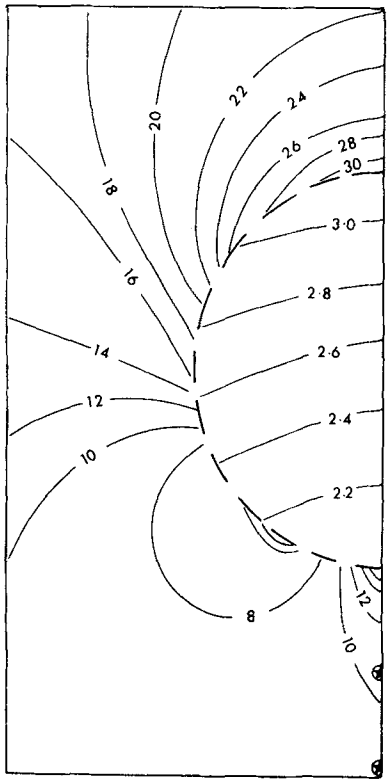

FIG. 9. Contours of the total-field bipole-dipole apparent resistivity (in $\Omega \cdot$ m) near a hemispherical sink for the bipole source placed radially with respect to the hemisphere. The model is described in Figure 8.

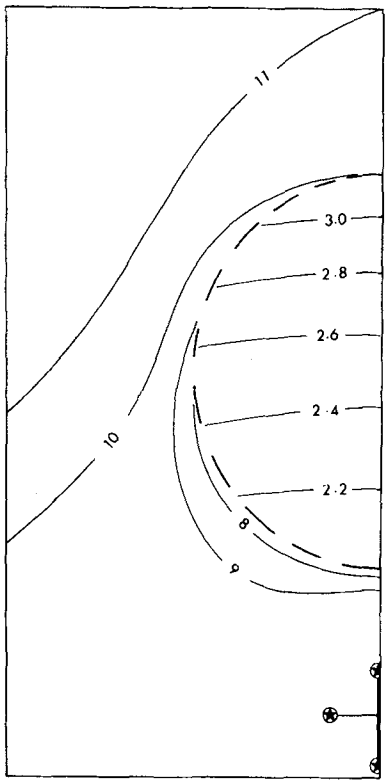

FIG. 11. The contours of the P_2 apparent resistivity invariant (in $\Omega \cdot$ m) for a multiple current bipole source in the presence of a hemisphere of low resistivity. The model is described in the caption to Figure 8. The values of P_2 outside the hemisphere closely reflect the resistivity of that region.

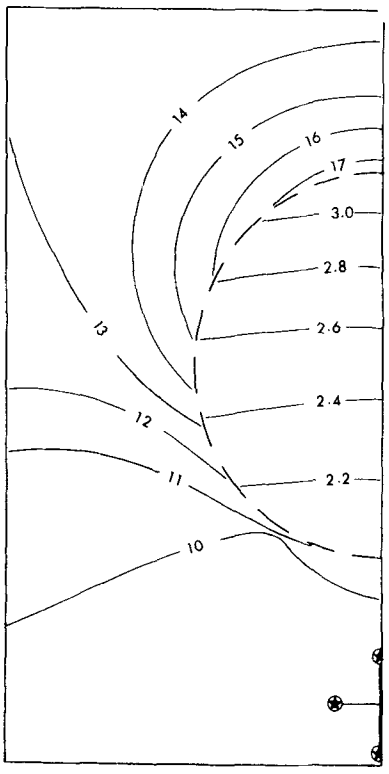

FIG. 10. Contours of the P_1 apparent resistivity invariant (in $\Omega \cdot$ m) for a multiple current bipole source in the presence of a hemisphere of low resistivity. The model is described in Figure 8.

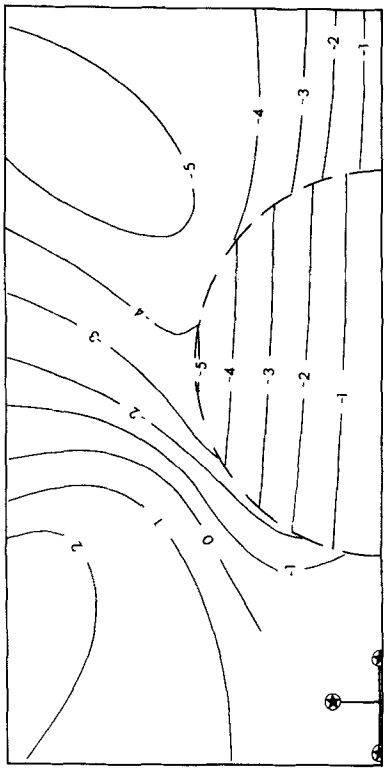

FIG. 12. Contours of the rotational invariant β in degrees for the model of Figure 8. Values are asymmetric about the diameter through the center of the current source.

ty or inaccuracies of measurement will result in near-random orientation of the maximum and minimum, rather than the consistent orientation seen in this model.

With near-isotropic apparent resistivity within the hemisphere, equation (37) suggests that just outside the boundary, large apparent anisotropy would be expected, with the maximum value of resistivity occurring when the electric field is perpendicular to the discontinuity. This is demonstrated in the plot of the apparent resistivity maximum and minimum (Figure 13) which shows high apparent anisotropy near the boundary, gradually diminishing with distance away from the hemisphere. The extreme values (the axes of the apparent resistivity ellipse) are a useful diagnostic tool in interpretation of multiple-source electrical surveys.

CONCLUSION

The apparent resistivity tensor method of analysis of multiple source bipole-quadripole surveys provides a means to incorporate all information from two or more separate bipole-quadripole surveys into a single representation. From the apparent resistivity tensor it is possible to derive any of the "mean" apparent resistivities previously suggested for combining multiple-source surveys. Thus, the quadripole-quadripole apparent resistivity of Doicin (1976) is one of the invariants of the tensor. Similarly, the parameters of the Keller and Furgerson (1977) "rotating dipole" method can be derived exactly from the tensor.

To analyze survey data, the apparent resistivity tensor can be broken down into invariants which highlight the particular objectives of the survey. This procedure eliminates the influence of the individual current source orientations and overcomes one of the major limitations of the bipole-dipole resistivity surveying technique. The invariants also give a better representation of resistivity below the measurement site than the representation obtained from either of the results from the separate bipole sources from which the tensor is derived. For a single vertical discontinuity in resistivity, the invariant P_1 takes values that closely approximate the resistivity under the measurement sites, and as the boundary is approached, this becomes exact. However, for a hemispherical model, the P_2 invariant is a better approximation.

The tensor method is particularly powerful for locating surface discontinuities in resistivity. Because the electric field perpendicular to the discontinuity is discontinuous, the change in the apparent resistivity tensor across a lateral change in resistivity is predominantly in the component orthogonal to the discontinuity. In the models studied here, this results in large apparent anisotropy in the vicinity of the resistivity change, with the greatest value of the total-field apparent resistivity occurring when the electric field is perpendicular to the discontinuity. The extreme values derived from the apparent resistivity tensor can thus be used to locate a near-surface resistivity change and to give an estimate of the orientation of the contact.

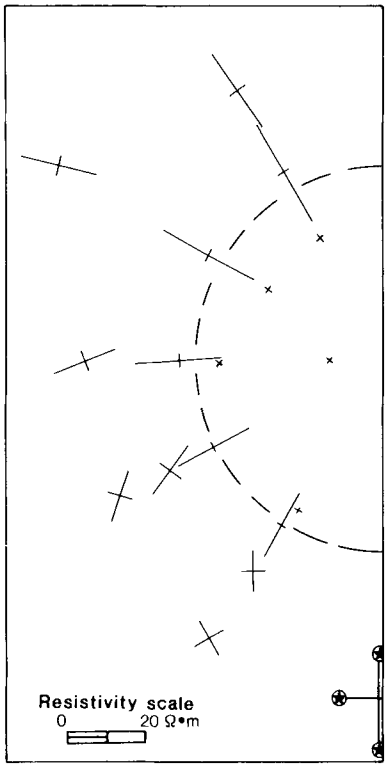

FIG. 13. The maximum and minimum apparent resistivities plotted at the azimuth of the corresponding electric field vector for a multiple-current bipole source in the presence of a low-resistivity hemispherical sink. The lengths of the bars are proportional to the resistivity. Note that at the boundary the azimuths of the maxima are perpendicular to the discontinuity in resistivity.

ACKNOWLEDGMENTS

Many people within Geophysics Division have contributed directly or indirectly with the development of the ideas presented. In particular, I acknowledge the contribution of G. F. Risk through many discussions of the techniques described and of their application. Thanks also to G. Caldwell (Auckland University), G. F. Risk, and W. J. P. Macdonald for their reviews of the manuscript.

REFERENCES

Al'pin, L. M., 1950, The theory of dipole sounding: Moscow, Gostophtekhizdat; (translation, Dipole methods for measuring earth conductivity 1966: Plenum Press, 1–60).

Anderson, L. A., and Keller, G. V., 1966, Experimental deep resistivity probes in the central and eastern United States: Geophysics, **31**, 1105–1122.

Beyer, J. H., 1977, Telluric and D. C. resistivity techniques applied to the geophysical investigation of Basin and Range geothermal systems: Ph.D. thesis, Univ. of California, Berkeley.

Bibby, H. M., 1977, The apparent resistivity tensor: Geophysics, **42**, 1258–1261.

Bibby, H. M., and Risk, G. F., 1973, Interpretation of dipole-dipole resistivity surveys using a hemispheroidal model: Geophysics, **38**, 719–736.

Bibby, H. M., Dawson, G. B., Rayner, H. H., Stagpoole, V. M., and Graham, D. J., 1984, The structure of Mokai geothermal field based on geophysical observations: J. Volcan. and Geotherm. Res., **20**, 1–20.

Dey, A., and Morrison, H. F., 1977, An analysis of the bipole-dipole method of resistivity surveying: Geothermics, **6**, 47–81.

Doicin, D., 1976, Quadripole-quadripole arrays for direct current resistivity measurements—Model studies: Geophysics, **41**, 79–95.

Frohlich, R. K., 1968, The influence of lateral inhomogeneities on the dipole methods: Geophys. Prosp., **16**, 314–325.

Habberjam, G. M., 1967, On the application of the reciprocity theorem in resistivity prospecting: Geophysics, **32**, 918–919.

Harthill, N., 1978, A quadripole resistivity survey of the Imperial Valley, California: Geophysics, **43**, 1485–1500.
Hohmann, G. W., and Jiracek, G. R., 1979, Bipole-dipole interpretation with three-dimensional models: Earth Science Laboratory, Univ. of Utah.
Keller, G. V., and Frischknecht, F. C., 1966, Electrical methods in geophysical prospecting: Pergamon Press.
Keller, G .V., Furgerson, R. B., Lee, C. Y., Harthill, N., and Jacobson, J. J., 1975, The dipole method: Geophysics, **40**, 451–472.
Keller, G. V., and Furgerson, R. B., 1977, Determining the resistivity of a resistant layer in the crust: Am. Geophys. Union Geophysics Monograph 20, 440–469.
Morris, D., 1978, A quadripole resistivity survey north of Gerlach, Nevada: Quart. J. Colorado School of Mines, **73**, 1–18.
Risk, G. F., Macdonald, W. J. P., and Dawson, G. B., 1970, D.C. resistivity surveys of the Broadlands geothermal region, New Zealand: Geothermics, Special Issue 2, **2**, 287–294.
Risk, G. F., Rayner, H. H., Stagpoole, V. M., Graham, D. J., Dawson, G. B., and Bennie, S. L., 1984, Electrical resistivity survey of the Wairakei geothermal field: Geophysics Div. Rep. no. 200, Dept. of Scientific and Industrial Research, Wellington.
Singh, S. K., and Espindola, J. M., 1976, Apparent resistivity of a perfectly conducting sphere buried in a half-space: Geophysics, **41**, 742–751.
Stanley, W. D., Jackson, D. B., and Zohdy, A. A. R., 1976, Deep electrical investigations in the Long Valley geothermal area, California: J. Geophys. Res., **85**, 810–820.
Tasci, M. T., 1975, Exploration for a geothermal system in the Lualualei Valley, Oahu, Hawaii: Grose, L. T. and Keller, G. V., Eds., Geothermal energy in the Pacific Region, Appendix A, Colorado School of Mines.
Van Nostrand, R. G., and Cook, K. L., 1966, Interpretation of resistivity data: U.S. Geol. Surv. Professional Paper 499.
Wenner, F., 1912, The four terminal conductor and the Thompson bridge: U.S. Bureau of Standards Bull., **8**, 559–610.
Zohdy, A. A. R., 1970, Geometric factors of bipole-dipole arrays: U.S. Geol. Surv. Bull. 1313B.
——— 1978, Total field resistivity mapping and soundings over horizontally layered media: Geophysics, **43**, 748–766.
Zohdy, A. A. R., and Jackson, D. B., 1969, Application of deep electrical soundings for groundwater exploration in Hawaii: Geophysics, **34**, 584–600.